

# Electrohydrodynamic (EHD) Enhancement of Boiling Heat Transfer of R113+WT4% Ethanol

Si-Doek Oh

Power and Industrial Systems R&D Center, Hyosung Corporation,  
Seoul 137-060, Korea

Ho-Young Kwak\*

Mechanical Engineering Department, Chung-Ang University,  
156-756, Korea

Nucleate boiling heat transfer for refrigerants, R113, and R113+wt4% ethanol mixture, an azeotropic mixture under electric field was investigated experimentally in a single-tube shell/tube heat exchanger. A special electrode configuration which provides a more uniform electric field that produces more higher voltage limit against the dielectric breakdown was used in this study. Experimental study has revealed that the electrical charge relaxation time is an important parameter for the boiling heat transfer enhancement under electric field. Up to 1210% enhancement of boiling heat transfer was obtained for R113+wt4% ethanol mixture which has the electrical charge relaxation time of 0.0053 sec whereas only 280% enhancement obtained for R113 which has relaxation time of 0.97 sec. With artificially machined boiling surface, more enhancement in the heat transfer coefficient in the azeotropic mixture was obtained.

**Key Words:** Azeotropic Mixture, EHD, Electrical Charge Relaxation Time, Nucleate Boiling

## Nomenclature

$A$  : Heat transfer area,  $m^2$   
 $C_p$  : Specific heat of water,  $kJ/kgK$   
 $D_b$  : Bubble diameter,  $m$   
 $E$  : Electric field strength,  $N/C$   
 $f_b$  : Frequency of bubble departure,  $1/s$   
 $g$  : Gravitational acceleration,  $m/s^2$   
 $h$  : Heat transfer coefficient,  $W/m^2K$   
 $I$  : Current,  $A$   
 $\dot{m}$  : Mass flow rate of water inside tube,  $kg/s$   
 $P$  : Pressure  
 $\dot{Q}$  : Heat flow rate,  $kJ/s$   
 $Re$  : Reynolds number  
 $R_m$  : Weighting factor defined by Eq. (4)  
 $T$  : Temperature,  $K$

$T_{as}$  : Average temperature of tube wall,  $K$   
 $V$  : Voltage

## Greek letters

$\epsilon$  : Permittivity constant,  $C^2/N^2-m^2$   
 $\rho$  : Density,  $kg/m^3$   
 $\sigma$  : Surface tension,  $N/m$   
 $\tau_b$  : Bubble departure time  
 $\tau_e$  : Electrical charge relaxation time

## Subscripts

$E$  : Electric field  
 $l$  : Liquid  
 $o$  : Zero field  
 $sat$  : Saturated state  
 $v$  : Vapor  
 $wi$  : Water stream at the inlet of tube  
 $wo$  : Water stream at the outlet of tube

\* Corresponding Author,

E-mail : kwakhy@cau.ac.kr

TEL : +82-2-820-5278; FAX : +82-2-826-7464

Mechanical Engineering Department, Chung-Ang University, 156-756, Korea. (Manuscript Received July 9, 2005; Revised March 3, 2006)

## 1. Introduction

For utilizing low temperature waste heat source,

one of major tasks is to develop high performance heat exchanger. Especially compact evaporator is an important thermal component for the plants such as Organic Rankine Cycle engine and large scale heat pumps. Electrohydrodynamic (EHD) augmentation (Cooper, 1990) has been proved to be one of the most appropriate techniques to enhance nucleate boiling heat transfer in dielectric liquids which are suitable working fluids for the evaporator employed in waste heat recovery plants.

Previous experiments of EHD enhancement in boiling heat transfer have been done mainly on the film boiling regime (Choi, 1960; Markels and Durfee, 1964), where dramatic increase in heat transfer rate occurs. Such great enhancement is known to be due to the film destabilization caused by electrical forces acting on the vapor-liquid interface (Johnson, 1968). Fundamental research was done to investigate the nucleation mechanism in a cavity under an electric field (Cooper, 1990) and how the dielectrophoretic force due to the difference between the dielectric permittivity of the liquid and vapor phases in a nonuniform electric field (Bonjour and Verdier, 1960) affects the bubble behavior near the boiling surfaces, which in turn promotes the heat transfer rate. EHD enhancement up to a factor of ten has been obtained from a lo-fin tube with complete elimination of boiling hysteresis (Cooper, 1990). The disturbance of heat transfer layer due to the buoyancy driven motion of bubble trapped in weak field region of the lo-fin tube (Cooper, 1990; Han et al., 1999) was reported to be a cause which bring such dramatic enhancement in nucleate boiling heat transfer.

One of the common findings from the previous investigations on EHD enhancement of nucleate boiling is that the number of bubble increases while the diameter of bubble decreases as the electric field increases (Basu, 1973; Cooper, 1990; Kawahira et al., 1990; Ohadi et al., 1992). Another interesting observation from previous experiments is the bubble coalescing on the lower part of heat transfer tube surrounded by six wire electrodes with equal spacing (Kawahira et al., 1990; Ohadi et al., 1992; Seyed-Yagoobi et al., 1996). Proper

electrode configuration for the case of employing wire electrodes around the heat transfer tube is required to induce buoyancy driven bubble motion which, in turn, enhance the boiling heat transfer (Oh and Kwak, 2000). However it has been found that the relaxation time of electrical charge of liquid is also one of crucial parameters to determine the influence of the electric field on the bubble behavior (Ogata et al., 1992). That is, if the relaxation time is much longer than the bubble detachment period, which is the case of FC-72, the bubble behavior is not affected by presence of the electric field at all (Han et al., 1999). Investigation of flow boiling in an annular channel under applied dc electric field which causes a flow regime redistribution was also done (Bryan and Seyed-Yagoobi, 2000; Cotton et al., 2005).

In this study, the effect of dc electric field on nucleate boiling heat transfer for refrigerants, R113, and R113+wt4% ethanol mixture, an azeotropic mixture was investigated experimentally by using a single tube shell/tube heat exchanger. Wide range of the wall superheat for boiling action was controlled by the temperature of the water flowing inside tube. For working fluids, R113, and R113+wt4% ethanol mixture which have quite different charge relaxation time in order of magnitude scale were chosen. Effect of the wall superheat and applied electric field strength on the nucleate boiling heat transfer were tested in this study. Also the nucleate boiling heat transfer coefficient in the azeotropic mixture with an artificially machined tube was measured.

## 2. Experimental Apparatus and Procedures

### 2.1 Experimental apparatus

A schematic diagram of the EHD augmentation boiling heat transfer unit is shown in Fig. 1. The experimental unit consists of a single tube shell/tube evaporator ①, condensers ②, ③, constant temperature bath circulator ④, hot water storage tank ⑤, and high voltage supplier ⑥. The evaporator shell was made of stainless steel pipe of 150 mm inside diameter with two 125 mm diame-

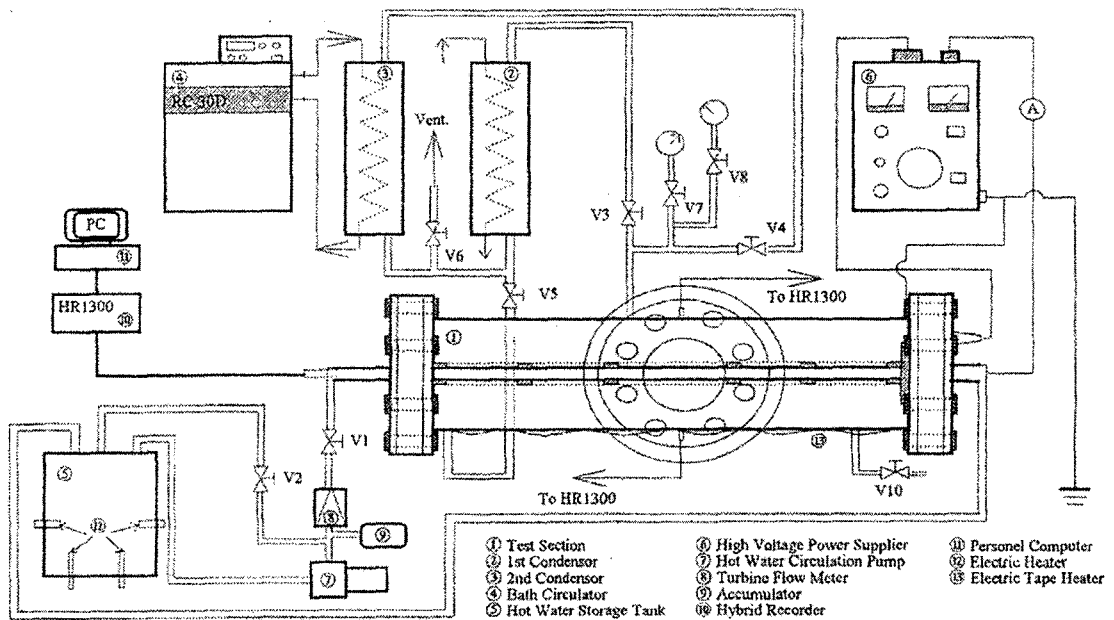


Fig. 1 Schematic diagram of experimental loop for boiling experiment

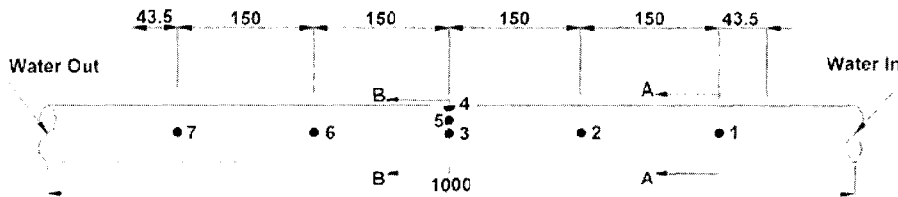


Fig. 2 Temperature measurement locations in the test tube (unit; mm)

ter sight glasses mounted at its midsection to facilitate visual observation of the bubble behavior on the boiling surface.

Hot water to the tube was supplied from an aluminum water tank. The water was heated by two 1 kW and four 100 W immersion heaters adjusted by variacs. Fine control of the water temperature in the tank was done by a temperature controller connected to four 100 W heaters. A friction pump (7) with mechanical seal delivered the hot water from the tank to the tube. Hot water flow rate modified by the bypass line was determined by means of a calibrated turbine flow meter (8) (Kobold Co., DF-48) in the liquid line. A diaphragm type accumulator (9) was installed in the liquid line to minimize the fluctuation in the flow rate. The vapor generated in the shell side tube was condensed and returned to the shell by

gravity. The cold water supplied from a constant temperature bath (4) was circulated into the cooling coil of the condenser. A detailed description for the test tube, and a method of installation of thermocouple junction on the test tube is in other papers (Han et al., 1999; Oh and Kwak, 2000). The tube wall temperatures were measured at five axial stations with equal intervals of 150 mm as shown in Fig. 2. Detailed method of embedding of the thermocouple junctions in the heater tube was described in Oh and Kwak (2000). Thermocouple junctions 3, 4, and 5 were used for the measurement of circumferential temperatures of the tube. The thermocouple junctions used were magnesium oxide insulation T-type sheathed with stainless steel tubing.

A schematic of the electrode configurations employed in this study is shown in Fig. 3. The

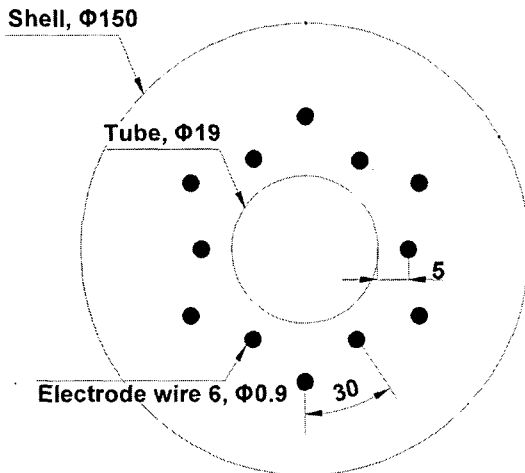


Fig. 3 Electrode configuration around test tube

first set of six electrodes which are oriented at  $60^\circ$  interval were located 5 mm away from the heating tube, while the other set of six electrodes placed between them were located 8 mm away from the tube. The electrode was made of 0.9 mm diameter carbon steel wire coated with copper. As can be seen in Fig. 1, these wires were supported and insulated from the shell and tube by six ring type teflon supporters fitted to the tube.

The calculated equipotential lines (a) and the direction of the dielectrophoretic force on a bubble (b) for the electrode configuration adopted in this study are shown in Fig. 4. As can be clearly seen in this figure (Fig. 4(b)), the dielectrophoretic force makes the bubbles on the heating surface move toward the electrostatic stagnation point between the electrodes. Also the electrode configuration adopted provides more uniform electric field (Fig. 4(a)), which increases the maximum voltage limit where dielectric breakdown occurs. Detailed calculation method for the electric field around electrodes and favorable configuration of the electrodes around the heated tube can be found in Oh and Kwak (2000). However, quite different bubble behavior under the non-uniform electric field generated by the mesh-type electrode may be plausible (Cooper, 1990).

A high voltage generator (Kilovolt Co., Model KV30-20) was utilized to supply high voltage up to 30 kV to the electrodes. Also a voltage regu-

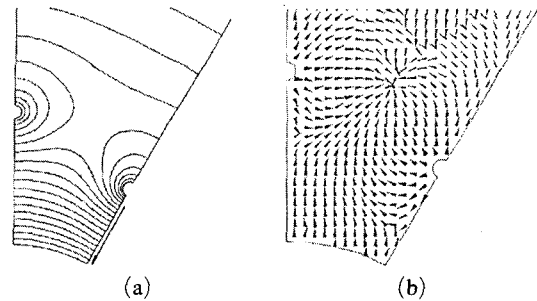


Fig. 4 Equipotential lines (a) and direction of dielectrophoretic force (b) for the electrode configuration adopted

lator was used to prevent dc ripples due to the change in the input ac voltage to the generator. The high voltage was fed into the EHD evaporator through a specially modified spark plug fitted in the teflon shell flange. The voltage and current to the electrode were measured by voltmeter (Fluke, 80K-40) and multimeter (Barnet Instrument Co., TS 352B/U), respectively.

## 2.2 Experimental procedures

For each run, degassing of the test liquid was performed by following procedure. After charging of the shell with working fluid, the wire heater winding around the shell was turned on and the hot water in the storage tank was circulated till the temperature of the test liquid reached at the predetermined value. This procedure was continued until the pressure inside the shell reaches 3 bar gauge due to the ebullition on the test tube surface. Then cold water was circulated in the condenser coil until the vapor generated in the shell was condensed to reduce the system pressure of 1 bar gauge. Next, the noncondensable gases were purged by opening the valve ⑥. The above procedures have been repeated several times for degassing.

The wall superheat of the tube was adjusted by changing the power supply to the immersion heaters installed in the storage tank. Detailed adjustment of the system pressure was done by controlling the cooling water flow rate and the temperature at the inlet of the condenser coil. If the temperature change of the vapor and liquid inside the shell are in the range of  $\pm 0.2^\circ\text{C}$ , the

system is assumed to have reached steady state. Once the steady state was established, the temperature and pressure of the system, the temperatures of hot water at inlet and outlet, the temperatures of tube wall and the voltage and current to the electrode were recorded.

For all cases, the boiling experiment at a particular wall superheat without electric field was performed first. Next, the high voltage was applied to the electrode. More detail experimental procedures are shown in Fig. 5. The saturation temperatures at the experimental conditions were 48.5°C for R113, R113 + wt4% ethanol mixture.

The flow rates of hot water, which is very important factor for achieving stable experimental condition, were 8 l/min for R113 and R113 + wt4% ethanol mixture. For completion of one set of experiments, ten hours or so were taken.

### 2.3 Data reduction

The heat transfer coefficient,  $h$  was determined by

$$h = \frac{\dot{Q}/A}{T_{as} - T_{sat}} \quad (1)$$

where  $T_{sat}$  is the saturation temperature of test liquid and  $A$  is the heat transfer area of the tube, which is approximately 0.0371 m<sup>2</sup>. The heat transfer rate to the working fluid inside the shell was assumed to be equal to the rate of energy loss of the hot water flowing inside the tube. This is given by

$$\dot{Q} = \dot{m} C_p (T_{wi} - T_{wo}) \quad (2)$$

The value of the specific heat of water,  $C_p$  was taken at the average temperature of bulk inlet and outlet temperatures of the water, i.e.  $(T_{wi} + T_{wo})/2$ . The average temperature of the tube wall,  $T_{as}$  was obtained by taking of the arithmetic mean of temperatures at the five side wall stations along the tube length with a weighting factor. That is

$$T_{as} = \frac{(T_1 + T_2 + T_3 + T_4 + T_5)}{5} \cdot TR_m \quad (3)$$

The weighting factor  $TR_m$  is just the ratio of the arithmetic mean temperatures measured at the three circumferential stations to the temperature at side wall, which is given by

$$TR_m = \frac{T_3 + 2T_4 + T_5}{4T_3} \quad (4)$$

Same circumferential temperature profile was assumed for all cross sections.

A typical way of obtaining the heat transfer coefficients is first to determine the local  $h$  based on local  $\Delta T$  and then take an average of all the local  $h$ 's to determine the heat transfer coefficient. However, the local heat flux is not defined here, which justifies our method to determine the heat transfer coefficients.

All T type thermocouples used were calibrated with dc voltage/current standard generator

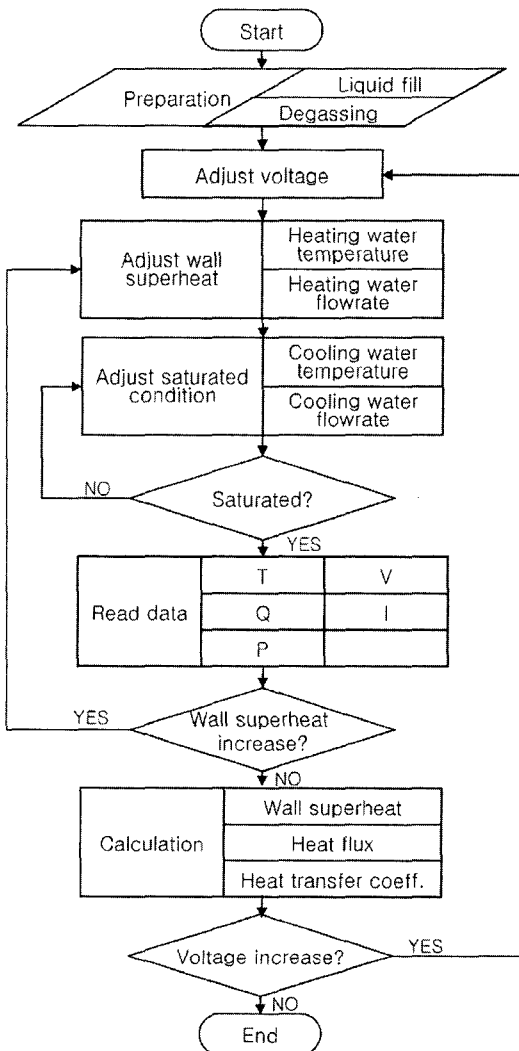


Fig. 5 Test procedure of boiling experiments

(Yokokawa, 2553) and semiconductor probe. Especially careful calibration was done for the thermocouples to measure the temperatures at the inlet and outlet of the test tube. In this case, the maximum calibrated temperature obtained was  $-0.3^{\circ}\text{C}$  at  $65^{\circ}\text{C}$  (Oh and Kwak, 2000). The acquisition of data obtained from the T type thermocouples was done by Yokokawa recorder (HR 1310) connected to PC. The data collected from each thermocouple in 2 minutes at 2 second interval were averaged separately to make a data set.

The uncertainties in the temperature measurements are less than  $\pm 0.1^{\circ}\text{C}$ , which yields a relative error of  $\pm 3.5\%$  for the measurements of the wall superheat,  $(T_{as} - T_{sat})$ . The uncertainties in the flow rate measurements are approximately  $\pm 2.5\%$ , so the calculated magnitudes of the heat fluxes are accurate within  $\pm 6.0\%$ . Consequently the uncertainty in measurement of the heat transfer coefficient given in Eq. (1) was calculated to be within  $\pm 9.5\%$ .

### 3. Characteristic Times Related to the Bubble Behavior Under Electric Field

It is well known that the bubble departure frequency is fundamentally related to the heat flux achieved in the boiling heat transfer (Judd and Hwang, 1976). The frequency which is essentially governed by buoyancy force and surface tension is given by the following equation.

$$f_b = \frac{1}{\tau_b} = C \left[ \frac{(\rho_l - \rho_v) g}{D_b \rho_l} \right]^{1/2} \quad (5)$$

For the refrigerants tested in this study, the bubble departure time,  $\tau_b$ , is about  $2 \times 10^{-2}$  s with  $C=0.56$ .

On the other hand, the charge relaxation time addition to the bubble departure time turns out to play a crucial role affecting the bubble behavior under electric field (Ogata et al., 1992). Under a homogeneous electric field with strength  $E$ , the electric charge generated at the interface are given by (Kawahira et al., 1990)

$$\rho_s = \epsilon E [1 - \exp(-\sigma t / \epsilon)] \quad (6)$$

**Table 1** Electric properties of test liquids and electrical charge relaxation times

Description	Electrical conductivity [A/Vm]	Dielectric constant	Charge Relaxation time [s]
Liquids		$8.86416 \times 10^{-12}$	
FC72	$1.00 \times 10^{-13}$	1.76	$1.56 \times 10^{+2}$
R113	$2.20 \times 10^{-11}$	2.41	$9.71 \times 10^{-1}$
R113+wt4% ethanol	$5.42 \times 10^{-9}$	3.27	$5.35 \times 10^{-3}$

The relaxation time which is solely related to the electrical properties of liquid can be obtained from Eq. (6)

$$\tau_e = \frac{\epsilon}{\sigma} \quad (7)$$

The characteristic time defined in Eq. (7) is considered as the time taken for an electric field to affect the bubble. Thus, the charge relaxation time of working fluid should be less than the bubble departure time for the electric field to affect the motion of the bubbles nucleated on the heating surface. In Table 1, the relaxation time of electrical charge for various refrigerants along with some electrical properties are shown.

### 4. Results and Discussions

For the refrigerants, FC72 tested by Han et al. (1999) with reference purpose, R113, and R113+wt4% ethanol mixture tested in this study, the boiling heat transfer coefficients as a function of the wall superheat with different applied voltages are shown in Figs. 6, 7, and 8 respectively.

Assuming that the electric force  $F_E$  acting on a bubble is purely dielectrophoretic, Barboi et al. (1968) successfully predicted the bubble departure diameter of bubbles in an electric field. The departure diameter obtained with electric field strength  $E$  at the heat transfer surface by considering a steady-state balance between electric, buoyancy and surface tension forces is given by

$$D_b = A(\theta) \left[ \frac{\sigma}{g(\rho_l - \rho_v)} \right]^{0.5} N_E \quad (8)$$

where  $A$  is a function of contact angle  $\theta$  and the electric influence number  $N_E$  such that

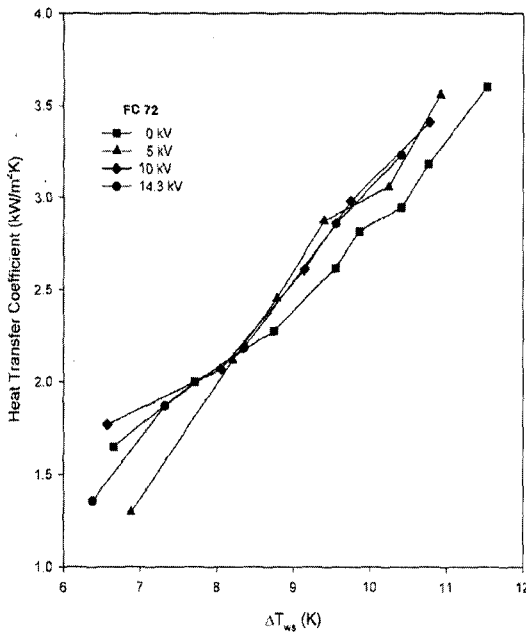


**Fig. 6** Variation of heat transfer coefficients for FC72 with six electrodes and  $Q_w=10$  l/min at  $T_s=57.5^\circ\text{C}$

$$N_E = \left( 1 + \frac{6|F_E|}{\pi g(\rho_l - \rho_v) D_b^3} \right)^{-0.5} \quad (9)$$

The dielectrophoretic force acting on a dielectric spherical bubble is given by (Snyder et al., 1996)

$$\vec{F} = \frac{\pi D_b^3 \epsilon_l (\epsilon_v - \epsilon_l)}{4(\epsilon_v + 2\epsilon_l)} \nabla E^2 \quad (10)$$

When an electric force acting on the bubble, or  $N_E$  being less than unity, the bubble departure diameter becomes smaller and consequently the bubble departure frequency becomes higher. Such argument explained by Eqs. (5) and (8) is in agreement with the previous experimental findings on the bubble behavior under electric field.

Cooper (1990) suggested the following correlation for the EHD enhancement of heat transfer by modifying the Rohsenow model for the nucleate boiling heat transfer (Rohsenow, 1952).

$$\frac{h_E}{h_o} = a N_E^{n/2} (\text{Re}_o)^b \quad (11)$$

where  $n=0.33$  as suggested by Rohsenow and where the constants  $a$  and  $b$  are determined empirically. However his data from EHD heat transfer of R114 on a horizontal lo-fin tube with

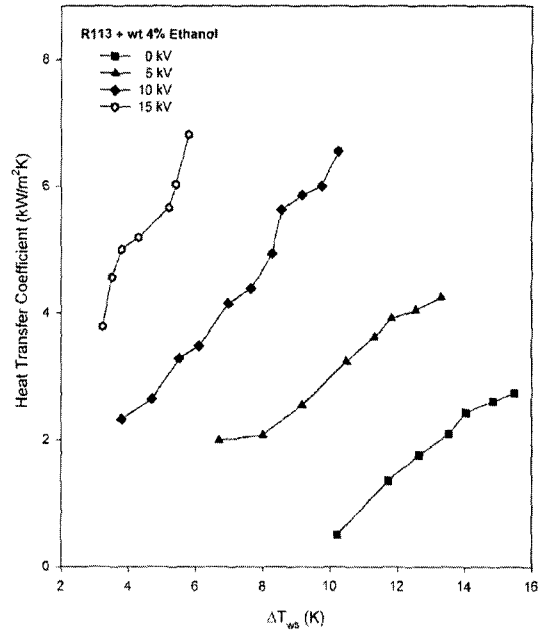


**Fig. 7** Variation of heat transfer coefficients for R113+wt4% ethanol with twelve electrodes and  $Q_w=8$  l/min at  $T_s=48.5^\circ\text{C}$

mesh-type cylindrical electrode could not be correlated with Eq. (11).

As shown in Fig. 6, the boiling heat transfer coefficients for FC72 increase slightly when voltage is applied. This may be attributed to much longer charge relaxation time of the fluid compared to the bubble departure one so that the electric field has little effect on the bubble motion. On the other hand, for R113+wt4% ethanol mixture whose charge relaxation time is shorter than the bubble departure time, great enhancement in the boiling heat transfer has been obtained as shown in Fig. 7. With a moderate applied voltage of 10 kV, the maximum heat transfer enhancement obtained is about 1210% at the wall superheat of 10 K. Certainly, such dramatic increase in the heat transfer coefficient for the nucleate boiling with an azeotropic mixture cannot be explained by Eqs. (8), (9) and (11). More general correlation for the EHD enhancement of heat transfer should be developed with considering the charge relaxation time.

Consequently it is not surprising that the EHD methodology yielded seven and half fold (750%)

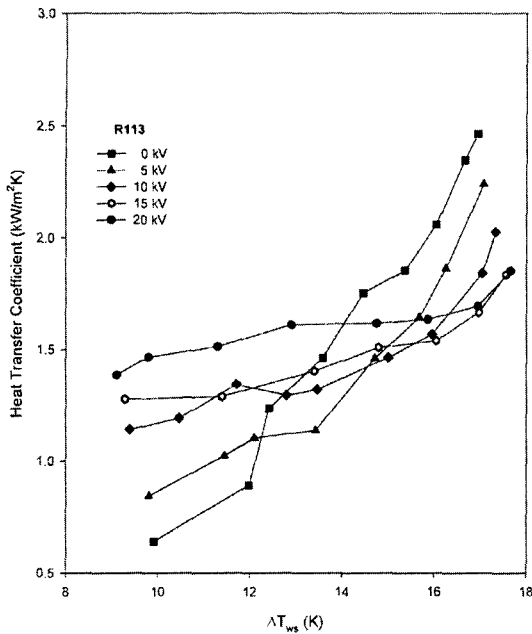


**Fig. 8** Variation of heat transfer coefficients for R113 with twelve electrodes and  $Q_w=8$  l/min at  $T_s=48.5^\circ\text{C}$

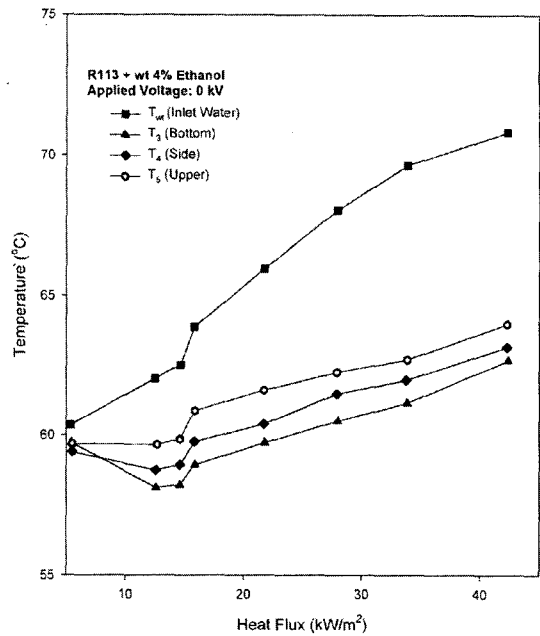


**Fig. 9** Variation of tube wall and inlet water temperature for different heat fluxes in R113+wt4% ethanol with twelve electrodes and  $Q_w=8$  l/min at  $T_s=48.5^\circ\text{C}$

increase in the heat transfer coefficients with HCFC-123 (Singh et al., 1993), a proposed substitute for R-11, having charge relaxation time of  $0.89 \times 10^{-3}$  s (Ogata et al., 1992). For a test of the heat transfer augmentation in the center of the bundle with the HCFC-123, Ogata et al. (1992) also obtained seven fold increase in the boiling heat transfer at an applied voltage of 18 kV.

Somewhat different results for R113 have been obtained. Abrupt increase when electric field is applied and thereafter no appreciable dependence on the wall superheat in the heat transfer coefficients at lower heat flux level have been found for R-113: However the boiling heat transfer coefficient achieved under electric field is lower than that for zero field if the wall superheat exceeds 13 K as shown in Fig. 8. This can be attributed to the fact that boiling action due to the buoyancy-driven force is suppressed by EHD force in the region where many bubbles form on the heating surface. Similar trend but slightly higher boiling heat transfer coefficients in R113 was obtained using the different electrode configuration consisting of six electrodes which are oriented at  $60^\circ$

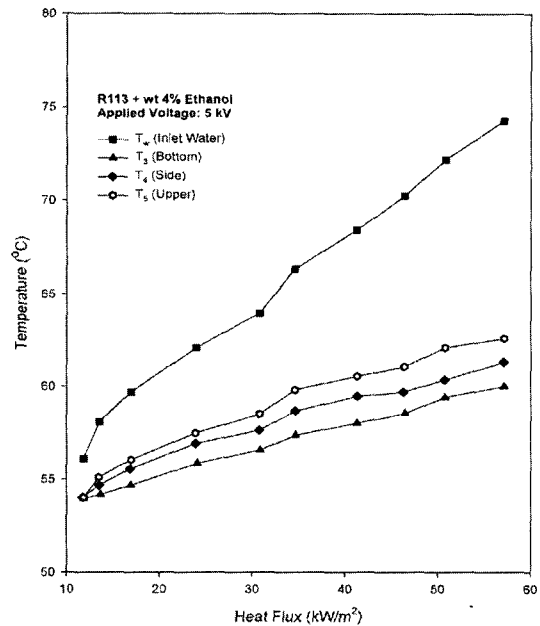


**Fig. 10** Variation of tube wall and inlet water temperature for different heat fluxes in R113+wt4% ethanol with twelve electrodes and  $Q_w=8$  l/min at  $T_s=48.5^\circ\text{C}$



intervals, and are located 5 mm away from the boiling surface. The electrode configuration where two electrodes are placed just below and above the boiling surface yields the best heat transfer coefficients (Oh and Kwak, 2000).

The variation of the circumferential temperatures at the midsection of the tube for different heat fluxes at zero voltage and the applied voltage of 5 kV are shown in Figs. 9 and 10 respectively. As shown in Fig. 9, the temperature drops at the tube wall especially at the bottom of the tube is noticeable as nucleate boiling starts. However, such boiling hysteresis is eliminated completely when the moderate voltage of 5 kV is applied. The temperature drop due to the boiling onset was also found to be eliminated by applying moderate voltage in R11 (Oh and Kwak, 2000). It is noted that boiling nucleation in R113+wt4% ethanol mixture started at lower heat flux level than the case in R113.

As shown in Figs. 11 and 12, a machined surface turned out to be effective to promote the boiling heat transfer as well as eliminate the boiling hysteresis under electric field also. The modified surface was machined by making three conical cavities having mouth diameter of 0.5 mm and depth of 0.2 mm on the boiling surface per unit length (cm) and the surface was polished with emery paper of #600. A two to three fold increase in the boiling heat transfer coefficients with the machined tube has been obtained for R113+wt4% ethanol mixture when compared to a plane one with the same electric field strength applied. It is demonstrated in these figures that compound EHD enhancement methodology with artificially machined surface yields highest enhancement at the lowest heat flux levels.

It should be noted that exotic boiling behavior of an azeotropic mixture under electric field has been observed, which needs further study. As shown in Fig. 13, a photographic study has revealed that the bubble patches generated on the boiling surface change their position sporadically for R113+wt4% ethanol mixture, which may be regarded as one of boiling characteristic for azeotropic mixture. This behavior is more strongly occurred as the applied electric field strengths

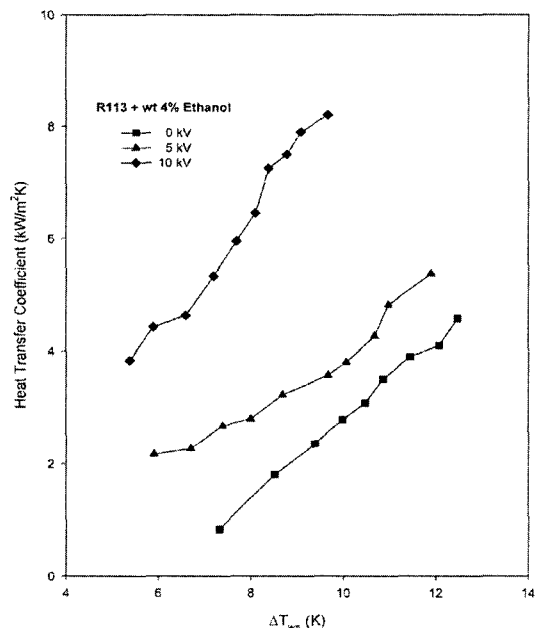


Fig. 11 Variation of heat transfer coefficients for R113 + wt4% ethanol with twelve electrodes, artificially machined tube and  $Q_w=8$  l/min at  $T_s=48.5^\circ\text{C}$

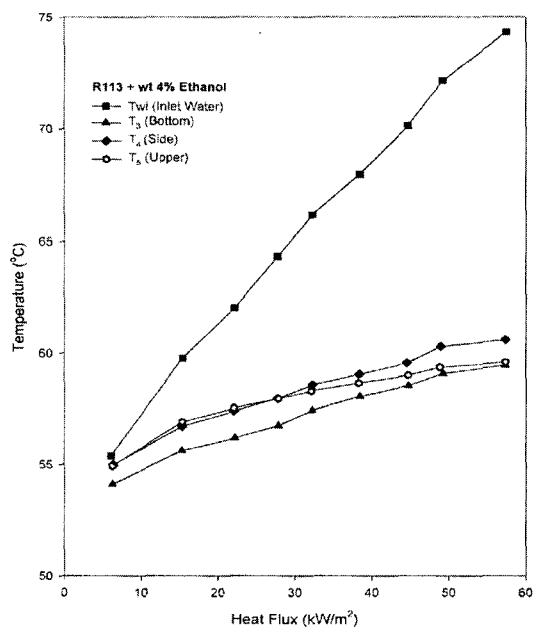
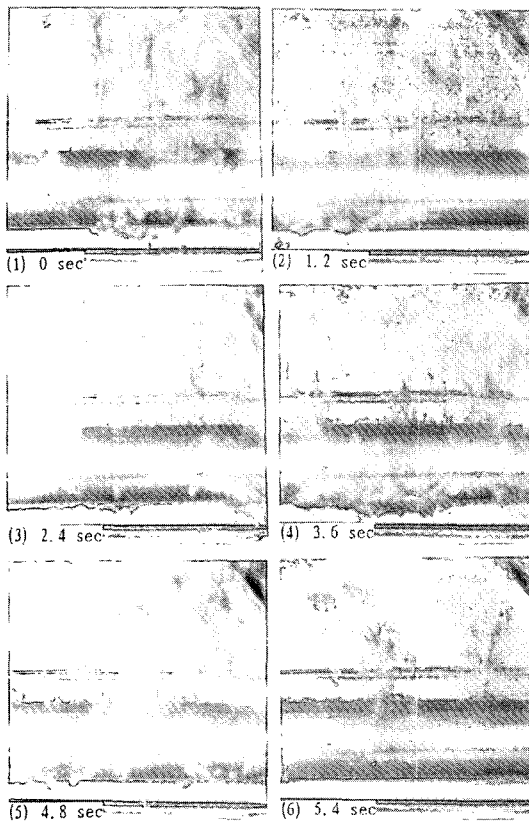


Fig. 12 Variation of tube wall and inlet water temperature for different heat fluxes in R113 + wt4% ethanol with twelve electrodes, artificially machined tube and  $Q_w=8$  l/min at  $T_s=48.5^\circ\text{C}$



**Fig. 13** Transient bubble behavior in R113+wt4% ethanol with twelve electrodes, 22.9 kW/m<sup>2</sup> and  $Q_w=8$  l/min at  $T_s=48.5^\circ\text{C}$

increase. Such sporadic patch boiling was not occurred in R113 (Oh and Kwak, 2000).

## 5. Conclusions

Effect of electric fields on boiling heat transfer for R113, and R113+wt4% ethanol mixture has been investigated experimentally. For R113+wt4% ethanol mixture, an azeotropic mixture, whose charge relaxation time is shorter than the bubble departure time, the maximum heat transfer enhancement obtained is about 1210% with application of a moderate voltage of 10 kV. On the other hand, only 280% enhancement in the boiling heat transfer coefficient was obtained for R113, which demonstrates that the charge relaxation time is an important parameter for EHD augmentation of boiling heat transfer. Experimental results have also revealed that compound

EHD enhancement methodology with artificially machined surface yields the highest enhancement at the lowest heat flux levels.

## Acknowledgments

This research was supported by The Chung-Ang University Research grant in 2005.

## References

- Basu, D. K., 1973, "Effect of Electric Fields on Boiling Hysteresis in Carbon Tetrachloride," *Int. J. Heat Mass Transfer*, Vol. 16, pp. 1322~1324.
- Bonjour, E. and Verdier, J., 1960, "Mecanisme de L'ebullition Sous Champ Electrique," *C. R. Hebd, Seasons Acad. Sci., Paris*, pp. 924~926.
- Bryan, J. E. and Seyed-Yagoobi, J., 2000, "Electrohydrodynamically Enhanced Convective Boiling: Relationship between Electrohydrodynamic Pressure and Momentum Flux Rate," *J. Heat Transfer*, Vol. 122, pp. 266~277.
- Cotton, J., Robinson, A. J., Shoukri, M. and Chang, J. S., 2005, "A Two-phase Flow Pattern Map for Annular Channels Under a DC Applied Voltage and the Application to Electrohydrodynamic Convection Boiling Analysis," *Int. J. Heat Mass Transfer*, Vol. 48, pp. 5563~5579.
- Cooper, P., 1990, "EHD Enhancement of Nucleate Boiling," *ASME J. Heat Transfer*, Vol. 112, pp. 458~464.
- Han, S., Na, M., Oh, S. and Kwak, H., 1999, "Electrohydrodynamic (EHD) Enhancement of Boiling Heat Transfer with a Lo-fin Tube," *KSME Int. J.*, Vol. 13, pp. 376~385.
- Johnson, R. L., 1968, "Effect of an Electric Field on Boiling Heat Transfer," *AIAA J.*, Vol. 6, pp. 1456~1460.
- Judd, R. L. and Hwang, K. S., 1976, "A Comprehensive Model for Nucleate Pool Boiling Heat Transfer Including Microlayer Evaporation," *ASME J. Heat Transfer*, Vol. C98, pp. 623~629.
- Kawahira, H., Kubo, Y., Yokoyama, T. and Ogata, J., 1990, "The Effect of an Electric Field on Boiling Heat Transfer of Refrigerant-11; Boiling on a Single Tube," *IEEE Trans. Ind. Appl.*, Vol. 26, pp. 359~365.

Markels, M. and Durfee, R. L., 1964, "The Effect of Applied Voltage on Boiling Heat Transfer," *AIChE J.*, Vol. 10, pp. 106~110.

Ogata, J., Iwafuji, Y., Shimada, Y. and Yamazaki, T., 1992, "Boiling Heat Transfer Enhancement in Tube-bundle Evaporators Utilizing Electric Field Effects," *ASHRAE Trans.: Symposia*, pp. 435~444 (BA-92-5-2).

Oh, S. and Kwak, H., 2000, "A Study of Bubble Behavior and Boiling Heat Transfer Enhancement Under Electric Field," *Heat Transfer Engineering*, Vol. 21, pp. 33~45.

Ohadi, M. M., Paper, R. A., Ng, T. L., Faani, M. A. and Radermacher, R., 1992, "EHD Enhancement of Shell-side Boiling Heat Transfer Coefficients of R-123/oil Mixture," *ASHRAE Trans. Symp.*, pp. 427~434 (BA-92-5-1).

Rohsenow, W. M., 1952, "A Method of Cor-

relating Heat Transfer Data for Surface Boiling of Liquids," *Trans. ASME* Vol. 74, pp. 969~976.

Seyed-Yagoobi, J., Geppert, C. A. and Geppert, L. M., 1996, "Electrohydrodynamically Enhanced Heat Transfer in Pool Boiling," *J. Heat Transfer*, Vol. 118, pp. 233~237.

Singh, A., Kumar, A., Dessiatoun, S., Faani, M.A., Ohadi, M.M. and Ansari, A.I., 1993, "Compound EHD-enhanced Pool Boiling of R-123 in a Liquid-to-Refrigerant Heat Exchanger," Paper #93-WA/HT-40, ASME.

Snyder, T. J., Schneider, J. B. and Chung, J. N., 1996, "A Second Look at Electrokinetic Phenomena in Boiling," *J. Appl. Phys.*, Vol. 79, pp. 6755~6760.

van Stralen, S. and Cole, R., 1979, *Boiling Phenomena*, Hemisphere Publishing Corp., New York.